Emergent quantum correlations and collective behavior in noninteracting quantum systems subject to stochastic resetting

Matteo Magoni [1], Federico Carollo [1], Gabriele Perfetto [1], and Igor Lesanovsky [1,2]

[1] *Institut für Theoretische Physik, Eberhard Karls Universität Tübingen, Auf der Morgenstelle 14, 72076 Tübingen, Germany*

[2] *School of Physics and Astronomy and Centre for the Mathematics and Theoretical Physics of Quantum Non-Equilibrium Systems, The University of Nottingham, Nottingham NG7 2RD, United Kingdom*

(Received 7 March 2022; accepted 31 October 2022; published 16 November 2022)

We investigate the dynamics of a noninteracting spin system, undergoing coherent Rabi oscillations, in the presence of stochastic resetting. We show that resetting generally induces long-range quantum and classical correlations both in the emergent dissipative dynamics and in the nonequilibrium stationary state. Moreover, for the case of conditional reset protocols—where the system is reinitialized to a state dependent on the outcome of a preceding measurement—we show that in the thermodynamic limit, the spin system can feature collective behavior which results in a phenomenology reminiscent of that occurring in nonequilibrium phase transitions. The discussed reset protocols can be implemented on quantum simulators and quantum devices that permit fast measurement and readout of macroscopic observables, such as the magnetization. Our approach does not require the control of coherent interactions and may therefore highlight a route towards a simple and robust creation of quantum correlations and collective nonequilibrium states, with potential applications in quantum enhanced metrology and sensing.

DOI: 10.1103/PhysRevA.106.052210

I. INTRODUCTION

Understanding and exploiting the interplay between coherent unitary evolution and measurement in quantum systems has been a central topic since the early days of quantum mechanics [1,2]. Recent research in this direction is closely linked to the physics of open quantum systems [3–6], where interactions among quantum particles compete with the coupling to the surrounding environment. Modern experiments allow one to externally control and even artificially engineer open system dynamics. This can, e.g., be achieved through so-called feedback protocols [7–12], which rely on the continuous monitoring of a system followed by some action conditioned on the output of a detector. This procedure can generate nonequilibrium steady states (NESS) that feature nontrivial quantum correlations [13–16]. Another approach that relies on externally imposed interventions in order to create effectively open system dynamics is *stochastic resetting* [17]. In its simplest form, it amounts to resetting a system to its initial state at random times. This procedure has been originally studied for classical diffusive systems [18–21], search processes [18,19,22–25], and active systems [26–32], and also here interesting NESS have been shown to emerge [33–44]. Similar observations have been made recently in the context of quantum systems [45–55]. However, it remains an open question whether resetting can induce nontrivial NESS, which may display emergent quantum correlations or even nonequilibrium phase transition behavior.

In this manuscript, we fill this gap by investigating the interplay between stochastic resetting and many-body quantum coherent evolution in the simplest—yet surprisingly nontrivial—case of noninteracting spin systems; see Fig. 1(a). We show that despite the absence of interactions in the coherent dynamics, resetting induces quantum correlations as well as a critical (nonanalytic) behavior in the NESS. We demonstrate this by envisaging three distinct protocols, named henceforth Protocol I, II, and III, in increasing order of complexity [see Figs. 1(b) and 1(c)]. Protocol I amounts to the aforementioned simple stochastic resetting of the system to a fixed state, while Protocols II and III include a measurement step whose outcome determines to which state the system is reset.

In *all three* cases, we find that resetting induces long-range correlations, although the system's reset-free dynamics is noninteracting. These correlations, emerging from the global operations associated with the reset events, are not exclusively of a statistical nature, but also have a quantum origin. Moreover, Protocols II and III induce stationary collective behavior, which manifests in nonanalyticities in an appropriate order parameter. While reminiscent of a nonequilibrium phase transition, the phenomenology we observe here is rather different in nature. Standard phase transitions take place between phases with short-range correlations and finite susceptibility parameter. Here, instead, due to the reset process, the system features strong long-range correlations and a divergent susceptibility throughout the whole phase diagram and not only at the critical point. The collectively enhanced response of the system to external parameter variations may be exploited for high-density quantum sensing, as discussed, e.g., in Refs. [56–58]. The fact that such property emerges even within a simple noninteracting system readily realizable with neutral atoms highlights a novel and simple way for creating

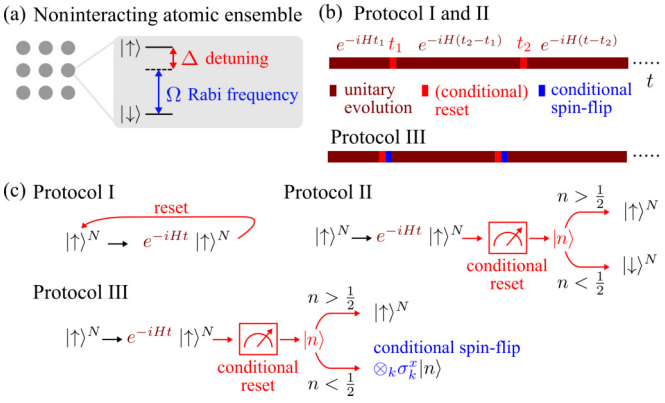

FIG. 1. Noninteracting spins subject to resetting. (a) Noninteracting spin system subject to a (laser) field with Rabi frequency Ω and detuning Δ. (b) The unitary time evolution according to Hamiltonian (1) is interspersed by randomly distributed reset events, which reinitialize the system to a specific state depending on the adopted reset protocol. In the figure, t denotes the observation time and t_k the time when the kth reset event takes place. (c) Details of the reset protocols. In Protocol I, the system is unconditionally reset to the state $|\uparrow\rangle^N$. In Protocols II and III, the reset is preceded by a measurement of the excitation density n, which selects a product configuration state $|n\rangle$, with density n. In Protocol II, the value of n determines the choice between two fixed reset states. In Protocol III, when $n < 1/2$, the reset state is determined by a spin-flip operation applied to the state obtained from the projective measurement.

and exploiting correlated many-body states on quantum simulators [59–63].

II. DYNAMICS AND RESET STATES

We consider a system of N spins with Hamiltonian

$$H = \Omega \sum_{i=1}^{N} \sigma_i^x + \Delta \sum_{i=1}^{N} \sigma_i^z, \tag{1}$$

describing, for instance, noninteracting atoms subject to an external laser field. Here, $\sigma_i^{x,y,z}$ are the Pauli matrices of the ith spin, Ω is the Rabi frequency, and Δ is the laser detuning. The two basis states of each spin, $|\uparrow\rangle$ and $|\downarrow\rangle$, are chosen as the eigenstates of σ^z and represent the excited state and the ground state, respectively [see Fig. 1(a)]. These can be, for example, two hyperfine levels of an atom or of an ion.

Before turning to the discussion of the reset protocols, it is useful to first characterize the dynamical properties of the system during its coherent evolution. Since Hamiltonian (1) is the sum of single-body terms, we can focus on the time evolution of single-body operators. For example, the local excitation density at site j, defined as $n_j = (1 + \sigma_j^z)/2$, evolves as $n_j^F(t) = e^{iH_j t} n_j e^{-iH_j t}$, with $H_j = \Omega\sigma_j^x + \Delta\sigma_j^z$ and F indicating evolution under the Hamiltonian reset-free dynamics. Without loss of generality, we fix the initial state to be $|\uparrow\rangle^N = \otimes_{i=1}^N |\uparrow\rangle_i$. With this choice, one finds $\langle n_j^F(t)\rangle_\uparrow = 1 - (\Omega^2/\overline{\Omega}^2)\sin^2(\overline{\Omega}t)$, where $\overline{\Omega} = \sqrt{\Omega^2 + \Delta^2}$ is the effective Rabi frequency and the arrow in the subscript indicates the initial state.

The reset protocols are depicted in Figs. 1(b) and 1(c). All have in common that the system evolves coherently with Hamiltonian (1) in between consecutive reset events. In Protocol I, we employ stochastic resetting, i.e., the system is reinitialized to the state $|\uparrow\rangle^N$ unconditionally to any measurement. In Protocols II and III, instead, the reset state is chosen conditionally on a measurement taken right before resetting, as pictured in Fig. 1(c). A natural choice for the quantity to be measured is the excitation density $n = (1/N)\sum_{i=1}^N n_i$. In particular, in Protocol II, first proposed in Ref. [51], two reset states are present, $|\uparrow\rangle^N$ and $|\downarrow\rangle^N$, which correspond to the two completely polarized states with excitation density 1 and 0, respectively. The outcome of the measurement determines the reset state: if the measured excitation density exceeds a certain threshold, which is fixed to be $1/2$, then the system is reset to $|\uparrow\rangle^N$; otherwise it is reset to $|\downarrow\rangle^N$. In Protocol III, the system is reset to $|\uparrow\rangle^N$ if the measured density exceeds the threshold. Otherwise, the coherent dynamics resumes from the state obtained by flipping all the spins in the postmeasurement configuration, as sketched in Fig. 1(c).

III. PROTOCOL I: UNCONDITIONAL RESET

In this simple case, the coherent dynamics of the system is interrupted at random times at which the system is reset to state $|\uparrow\rangle^N$. Resets happen at a constant rate γ. The time τ between consecutive reset is therefore distributed according to the Poisson waiting time distribution $f(\tau) = \gamma e^{-\gamma\tau}$ (see Appendix E for a different waiting time distribution). The survival probability, i.e., the probability that no reset happens for a time τ, is given by $q(\tau) = \int_\tau^\infty f(s)ds = e^{-\gamma\tau}$. This, together with the reset-free time-evolved density matrix $\rho_\uparrow^F(t)$, determines the quantum state of the system $\rho_\uparrow(t)$ in the presence of resetting through the *last renewal* equation derived in Ref. [48],

$$\rho_\uparrow(t) = e^{-\gamma t}\rho_\uparrow^F(t) + \gamma \int_0^t dt' e^{-\gamma t'} \rho_\uparrow^F(t'). \tag{2}$$

The first term in the above equation corresponds to having no reset up to time t. The second term accounts for realizations of the stochastic resetting process where the last reset has been at a previous time $t - t'$ and the system has then evolved without reset events up to time t via the Hamiltonian (1).

The average excitation density in state (2) is given by $\langle n(t)\rangle_\uparrow = \mathrm{Tr}[n\rho_\uparrow(t)]$ and its stationary value reads

$$\langle n\rangle_{\uparrow,\mathrm{ness}} = \lim_{t\to\infty} \langle n(t)\rangle_\uparrow = 1 - 2\frac{\Omega^2}{\gamma^2 + 4\overline{\Omega}^2}, \tag{3}$$

which is shown in Fig. 2(a). This expression smoothly varies with Ω/Δ, contrary to what we will show for Protocols II and III. Equation (3) is equal to 1, i.e., the excitation density of the initial state, for $\Omega = 0$ (no coupling between single spin states), $\gamma \to \infty$ (the infinitely frequent resets induce a quantum Zeno effect [64,65] which freezes the system to its initial state), and $\Delta \to \infty$ (transitions between the two spins states are highly off-resonant). Note, finally, that the limit $\gamma \to 0$ corresponds to a stationary state with extremely rare reset events.

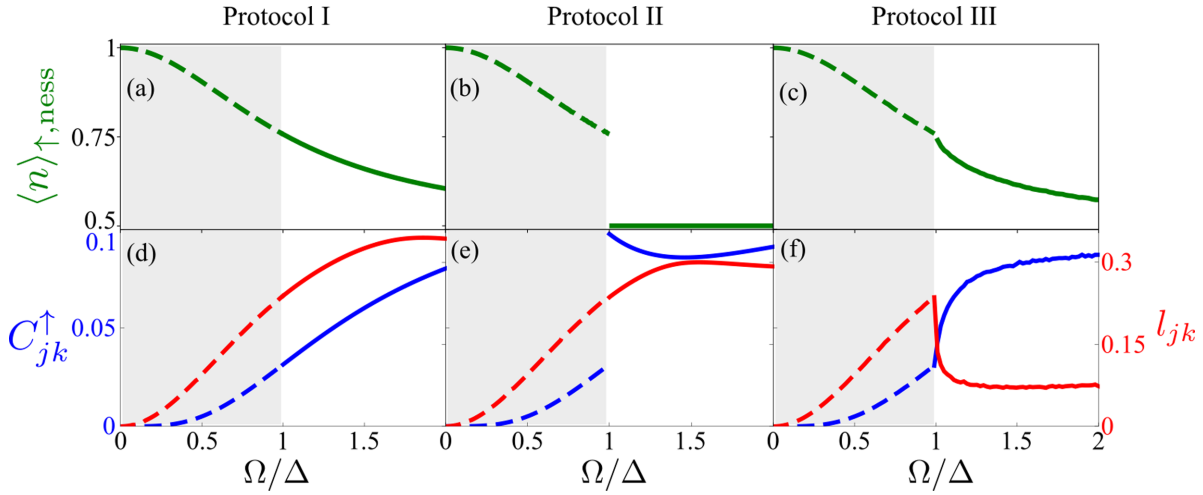

FIG. 2. Collective behavior and quantum correlations induced by reset. First row: stationary excitation density as a function of Ω/Δ for the three protocols. (a) For Protocol I, the order parameter (excitation density) is given by Eq. (3). For Protocols (b) II and (c) III, the order parameter displays a nonanalyticity at the critical point $\Omega_c = \Delta$, which is discontinuous or continuous, respectively. For Protocol III, the order parameter behaves as a power law when approaching the critical point from the right with an exponent close to 0.5. Second row: Connected correlation function (in blue, left axis) and quantum discord (in red, right axis), computed from the two-spin reduced density matrix ρ_{jk}, as a function of Ω/Δ. In contrast to (d) Protocol I, where both quantities are continuous, (e) Protocol II leads to a discontinuity of both quantities at the critical point $\Omega_c = \Delta$. Note that the discontinuity of the quantum discord is imperceptible on the scale shown. (f) For reset Protocol III, both the connected correlation function and the quantum discord feature power-law behavior in a right neighborhood of the critical point. The characteristic exponent is approximately 0.5 for the connected correlation function and 0.2 for the quantum discord. The dashed parts of the curves in all panels highlight the fact that when $\Omega < \Delta$, the three protocols become equivalent. All data are obtained analytically, except for (c) and (f) where numerical simulations are necessary. The reset rate is chosen to be $\gamma = \Delta/2$.

Rather surprisingly, although in each realization of the process the system is in a product state at all times, the reset mechanism introduces long-range correlations. This is due to the *global* character of the resetting procedure: all the individual spins are reset to the same single-spin state. This becomes evident when looking at the stationary two-spin connected correlation function $C^{\uparrow}_{jk} = [\langle n_j n_k \rangle_{\uparrow,\mathrm{ness}} - \langle n_j \rangle_{\uparrow,\mathrm{ness}} \langle n_k \rangle_{\uparrow,\mathrm{ness}}]$, which is equal to

$$C^{\uparrow}_{jk} = 4\Omega^4 \frac{5\gamma^2 + 8\overline{\Omega}^2}{(\gamma^2 + 4\overline{\Omega}^2)^2(\gamma^2 + 16\overline{\Omega}^2)}, \tag{4}$$

showing that correlations do not depend on the considered spins. This is reminiscent of what happens in fully connected models (see, e.g., [66] for an example in dissipative settings). However, in our case, these correlations are *strong* in the sense that they do not vanish in the thermodynamic $N \to \infty$ limit. As such, contrary to the case of fully connected models [67], the stationary state of our reset process is not clustering, i.e., it does not possess Gaussian fluctuations, as shown by the fact that the susceptibility is diverging: $\chi = \lim_{N\to\infty} 1/N \sum_{j,k=1}^{N} C^{\uparrow}_{jk} = \infty$. Note that the correlations (4) can also be computed from suitable single-spin trajectory correlations, following, e.g., Ref. [68]. This is, however, not possible for Hamiltonians with interactions among the spins or for the Protocols II and III discussed further below.

In addition to these strong classical density-density correlations, the NESS, in fact, also contain correlations of quantum origin. This aspect can be shown by computing the local quantum uncertainty (LQU), defined in Ref. [69], which is a type of bipartite quantum discord [70,71]. It quantifies the extent of the fluctuations of a local measurement due to the noncommutativity between the state and the measured local observable. The LQU isolates the fluctuations that are caused only by the coherence of the state and not by its mixedness. Despite being a fairly common feature in quantum states [72], quantum discord is proved to be a useful quantity for metrology and sensing applications [73–75]. Here we compute the LQU for the stationary two-spin reduced density matrix ρ_{jk}; see Appendix C. It is given by $l_{jk} = 1 - \lambda_{\max}\{W_{jk}\}$, where $\lambda_{\max}\{W_{jk}\}$ is the largest eigenvalue of the 3×3 matrix W_{jk} with elements $(W_{jk})_{ab} = \mathrm{Tr}[\sqrt{\rho_{jk}}(\sigma^a_j \otimes \mathbb{1})\sqrt{\rho_{jk}}(\sigma^b_j \otimes \mathbb{1})]$, with $a, b = x, y, z$. As for the classical correlations, the LQU also does not depend on the distance between sites. In Fig. 2(d), we show the connected correlation function (4) (left axis) together with the quantum discord quantified via the LQU (right axis) for Protocol I. Both quantities possess qualitatively the same shape and smoothly vary with Ω/Δ.

IV. PROTOCOL II: CONDITIONAL RESET TO TWO STATES

This protocol exploits two reset states: $|\uparrow\rangle^N$ and $|\downarrow\rangle^N$. At each reset event, the local density at each site is measured and the total excitation density n is computed. The system is reinitialized to the reset state $|\uparrow\rangle^N$ if the majority of the spins is found in the excited state, i.e., $n > 1/2$. On the contrary, if $n < 1/2$, the reset state is chosen as $|\downarrow\rangle^N$. For large N, the probability distribution for measuring a certain value of n after a time t since the last reset is a Gaussian distribution centered on the average, $\langle n^F(t)\rangle_{\uparrow/\downarrow}$, with variance

$\sigma_n^2 \propto 1/N$. This means that at each reset event, the system can, in principle, be reinitialized in both reset states, albeit with different probabilities. This aspect, together with the fact that the Hamiltonian dynamics of the average density satisfies the relation $\langle n^F(t)\rangle_\uparrow = 1 - \langle n^F(t)\rangle_\downarrow$, makes the stationary excitation density exactly equal to $1/2$, i.e., the average between the density of the two reset states; see Appendix B.

A different phenomenology takes place in the thermodynamic limit $N \to \infty$. In this case, as a consequence of the *law of large numbers* applied to the operator n, the probability distribution to measure a certain value for n becomes a δ function peaked around the average $\langle n^F(t)\rangle_{\uparrow/\downarrow}$. This self-averaging property makes the measurement of the excitation density fully deterministic with outcome equal to its average value. As a consequence, for $\Omega < \Delta$, given the initial condition and the fact that $\langle n^F(t)\rangle_\uparrow > 1/2 \ \ \forall t$, the system can only be reset to the state $|\uparrow\rangle^N$ and, therefore, the average density in the process is always larger than $1/2$. For $\Omega > \Delta$, instead, both reset states can be reached so that the stationary excitation density is equal to $1/2$; see Appendix B. The stationary excitation density, acting as an order parameter, then displays a jump discontinuity at the critical point $\Omega_c = \Delta$, as shown in Fig. 2(b). This is a consequence of an abrupt change in the dynamics: for $\Omega > \Delta$, the system can reset to both states, while for $\Omega < \Delta$, the dynamics is effectively that of Protocol I, with the stationary excitation density coinciding with Eq. (3) (see, also, Fig. 2).

As shown in Fig. 2(e), the connected correlation function and the quantum discord display a behavior that is qualitatively different from that of Protocol I. They are both discontinuous at the critical point even though the discontinuity of the LQU is tiny on the scale of the figure.

V. PROTOCOL III: CONDITIONAL RESET TO THE INITIAL STATE

In the third protocol, the system is reset to its initial state $|\uparrow\rangle^N$ only if the measured excitation density exceeds $1/2$. If not, the system resumes its dynamics from the state generated by the projective measurement after a subsequent flip of all its spins is performed [see Figs. 1(b) and 1(c)]. This means that if the state after the projective measurement possesses an excitation density equal to $n' < 1/2$, the reset state will have excitation density $1 - n' > 1/2$. This protocol is still conditioned on the measured excitation density, but, in contrast to Protocol II, any state with $n > 1/2$ can be considered as a reset state according to the parameter regime. The resulting nonequilibrium phase diagram [see Fig. 2(c)] exhibits a continuous nonanalytic behavior at the critical point $\Omega_c = \Delta$.

We note that without the additional spin-flip operation, the stationary behavior of the density would be discontinuous also for this protocol. Indeed, when $\Omega > \Delta$, each realization of the reset process would spend, on average, half of the time in configurations with n smaller than $1/2$ and half of the time in configurations with n larger than $1/2$. The stationary state, obtained by averaging over trajectories, would therefore be very different from the one attained when $\Omega < \Delta$, where trajectories maintain a positive magnetization, $n > 1/2$, throughout the whole reset process. This substantial dissimilarity between the two regimes would result in a jump discontinuity of the order parameter at Ω_c. On the contrary, with the introduction of the spin-flip operation, the order parameter is continuous, but still nonanalytic since its first derivative has a jump discontinuity at Ω_c. This can be understood by noticing that in this case, for $\Omega \gtrsim \Delta$, each trajectory of the reset process spends only an infinitesimal time in states with $n < 1/2$ since after a reset the system restarts the dynamics from a state with $n > 1/2$.

In the vicinity of Ω_c, the order parameter displays a power-law behavior $\sim (\Omega - \Omega_c)^\beta$, for $\Omega \to \Omega_c^+$, with a static exponent $\beta \approx 0.5$. This seems to indicate the emergence of a second-order phase transition in the NESS. However, looking at the behavior of the correlation function reveals a rather unexpected phenomenology. Indeed, in second-order phase transitions, upon approaching the critical point, the correlation length of the system increases, giving rise to a power-law divergence of the susceptibility at criticality. Here, instead, as already mentioned when discussing Protocol I, the system features strong long-range correlations which determine a divergence of the susceptibility parameter χ for any value of Ω/Δ and not only at criticality. Despite this divergence, we can still analyze the two-spin correlation function $C_{jk}^{\uparrow}$. This quantity, displayed in Fig. 2(f), interestingly also obeys a power-law behavior $\sim(\Omega - \Omega_c)^\beta$ close to the critical point, with the same static exponent β of the order parameter. Also, the quantum discord, as measured by the LQU, follows a power law with exponent $\delta \approx 0.2$.

VI. CONCLUSIONS AND OUTLOOK

We have shown that combining a noninteracting quantum dynamics with an externally imposed reset process can lead to surprisingly rich nonequilibrium stationary states. Even the simplest possible protocol results in a state with nontrivial classical and quantum correlations. More involved protocols lead to the emergence of a phase-transition behavior in an initially noninteracting system, which may be relevant for the implementation of quantum sensing and metrology applications [56,76–78]. The nonanalyticities characterizing such collective behavior emerge since the reset state is completely determined, in the thermodynamic limit, by the average value of the density as a consequence of the *law of large numbers*. For any finite system, fluctuations in the measurement outcomes inhibit the emergence of the observed nonanalyticities. We have shown how this occurs in the case of a noninteracting unitary dynamics. However, one would observe a similar phenomenology in the case of Hamiltonian dynamics with short-range interactions, for which the time evolution only builds up exponentially decaying correlations which do not invalidate the convergence of the operator n to its average value, in the large-N limit. Conceptually, this mechanism underlying collective behavior may appear simpler than the creation of strong coherent interactions. However, one requires the ability to rapidly read out and initialize the spin ensemble [79]. For the results discussed in Fig. 2, we have assumed a reset rate $\gamma = \Delta/2$, which in some settings may be impractical (it could be of the order of MHz for cold atoms). However, our findings do not change qualitatively for smaller values of the reset rate. The key quantity is indeed the ratio Ω/Δ, while the value of γ simply provides the timescale for the approach to stationarity.

ACKNOWLEDGMENTS

We acknowledge support from the "Wissenschaftler Rückkehrprogramm GSO/CZS" of the Carl-Zeiss-Stiftung and the German Scholars Organization e.V., from the European Union's Horizon 2020 research and innovation program under Grant Agreement No. 800942 (ErBeStA), as well as from the Baden-Württemberg Stiftung through Project No. BWST_ISF2019-23. We also acknowledge funding from the Deutsche Forschungsgemeinschaft through SPP 1929 (GiRyd), Grant No. 428276754, as well as through the Research Unit FOR 5413/1, Grant No. 465199066. G.P. acknowledges support from the Alexander von Humboldt Foundation through a Humboldt research fellowship for postdoctoral researchers.

APPENDIX A: GENERAL EXPRESSION OF THE STATIONARY DENSITY MATRIX FOR PROTOCOL II

The resetting dynamics described in Protocols I and II allows one to write the exact form of the stationary density matrix $\rho_{\rm ness}$ in terms of the waiting time distribution and the reset-free dynamical properties of the system. In particular, for Protocol II, the expression of the stationary density matrix $\rho_{\rm ness}$ has been determined in Ref. [51] and it reads

$$\rho_{\rm ness} = \frac{c_\uparrow}{\widehat{q}} \int_0^\infty dt' q(t') \rho_\uparrow^F(t') + \frac{c_\downarrow}{\widehat{q}} \int_0^\infty dt' q(t') \rho_\downarrow^F(t'), \tag{A1}$$

where

$$c_\uparrow = \frac{R_{\downarrow\uparrow}}{R_{\downarrow\uparrow} + R_{\uparrow\downarrow}}, \quad c_\downarrow = \frac{R_{\uparrow\downarrow}}{R_{\downarrow\uparrow} + R_{\uparrow\downarrow}}, \tag{A2}$$

and

$$\widehat{q} = \int_0^\infty dt' q(t'), \quad R_{ij} = \gamma \int_0^\infty dt' e^{-\gamma t'} P_{ij}(t'), \quad i, j = \uparrow, \downarrow . \tag{A3}$$

In the previous equation, $P_{ij}(t)$ is the probability that the system, starting its reset-free evolution from the reset state $|i\rangle$ ($|\uparrow\rangle^N$ or $|\downarrow\rangle^N$), in the occurrence of a reset event after a time t, is reinitialized to the reset state $|j\rangle$ ($|\uparrow\rangle^N$ or $|\downarrow\rangle^N$). Equation (A1) expresses $\rho_{\rm ness}$ as a statistical mixture of the unitary time evolutions ensuing from the reset states $|\uparrow\rangle^N$ and $|\downarrow\rangle^N$. Fundamentally, both weights $c_\uparrow$ and $c_\downarrow$ couple the Hamiltonian dynamics with the reset via Eqs. (A2) and (A3). In particular, since the probabilities $P_{ij}(t)$ depend on Ω, the weights $c_{\uparrow/\downarrow}$ also depend on Ω.

In the main text and further below in Appendices B–D, for the sake of simplicity, we consider the case of Poissonian resetting, with survival probability $q(t) = \exp(-\gamma t)$, while we comment in Appendix E about the non-Poissonian case.

For Protocol III, any state with excitation density $n > 1/2$ can be considered as a reset state. The generalization of Eq. (A1) is therefore of no practical utility since it involves a summation over all the reset states, whose number is exponentially large in the system size. In order to obtain the stationary values of different properties such as the excitation density, the two-point correlation function, and the quantum discord, in Protocol III, we shall therefore resort to Monte Carlo simulations and use combinatorial properties (see Appendix D).

We finally note that the expression in Eq. (A1) does not apply in the regime $\Omega < \Delta$, when considering the noninteracting spin system in the thermodynamic limit $N \to \infty$. Indeed, as we discuss below, for $\Omega < \Delta$, the magnetization of the spin ensemble can never change sign so that whether $n < 1/2$ or $n > 1/2$ throughout the whole dynamics solely depends on the value of n in the initial state. This implies that the system cannot visit all the reset states, as witnessed, for instance, by the fact that $P_{\uparrow\downarrow} = P_{\downarrow\uparrow} = 0$ for Protocol II (similar relations would apply to Protocol III). As such, the quantities $c_{\uparrow/\downarrow}$ become, in principle, ill defined. In any case, it is straightforward to see that starting from the state with all spins pointing up, in the regime $\Omega < \Delta$ and in the thermodynamic limit $N \to \infty$, the system can only reset to its initial state. As such, in this regime, the stationary density matrix is the one given in Eq. (A1) with $c_\uparrow = 1$ and $c_\downarrow = 0$. Note that in this limit, the stationary density matrix in Eq. (A1) reduces to the stationary limit of Eq. (2) in the main text, as expected. This applies to both Protocol II and Protocol III.

APPENDIX B: STATISTICAL PROPERTIES OF THE EXCITATION DENSITY IN A FINITE SYSTEM

From Appendix A, it is evident that once the probabilities $P_{ij}(t)$ in Eq. (A3) are computed, one can then easily obtain the stationary density matrix defined in Eq. (A1), which is valid for Protocol II. Exploiting the fact that the spins do not interact, it is indeed possible to compute those probabilities. Let us therefore focus on Protocol II, where the measurement of the excitation density n determines the reset state to choose. In particular, if the outcome of the measurement exceeds the threshold $1/2$, the selected reset state is $|\uparrow\rangle^N$; otherwise it is $|\downarrow\rangle^N$. It would therefore be beneficial to have an expression for the probability to measure a certain value of n which, at a given time t, is above or below this threshold. To compute this probability, it is of course sufficient to consider only the properties of the reset-free dynamics. The fact that the system is noninteracting reduces the computation to a simple combinatorial problem. Since the threshold is $1/2$, a sort of majority rule applies in the sense that the threshold is exceeded whenever there are more up spins than down spins.

As an example, let us show how to compute $P_{\uparrow\downarrow}^{(N)}(t)$, which is defined to be the probability that the system, being initialized in $|\uparrow\rangle^N$ (appearing as first subscript), is found after a time t to have an excitation density $n < 1/2$ (appearing as the second subscript). In the notation of Appendix A, it would be $P_{ij}(t)$, with $i = \uparrow$ and $j = \downarrow$. Following the majority rule, this amounts to the probability of having, after a time t, more down spins than up spins. Assuming, for simplicity, that the total number of spins, N, is odd and denoting with $p^{\uparrow\downarrow}(t) = (\Omega^2/\overline{\Omega}^2)\sin^2(\overline{\Omega}t)$ the probability that a single spin, initialized in the state $|\uparrow\rangle$, is found after a time t in the state $|\downarrow\rangle$,

$$P_{\uparrow\downarrow}^{(N)}(t) = \sum_{k=0}^{\frac{N-1}{2}} \binom{N}{k} [1 - p^{\uparrow\downarrow}(t)]^k [p^{\uparrow\downarrow}(t)]^{N-k}, \tag{B1}$$

which takes into account all the possible spin configurations with, at most, $(N-1)/2$ spins in the excited state. By using

the normal approximation of the binomial distribution, which is valid for large N (see, e.g., Ref. [80]),

$$\binom{N}{k}(1-p)^k p^{N-k} \simeq \frac{1}{\sqrt{2\pi N p(1-p)}} \exp\left[-\frac{[k-N(1-p)]^2}{2Np(1-p)}\right], \tag{B2}$$

and approximating the discrete sum with an integral, Eq. (B1) gets simplified to

$$P_{\uparrow\downarrow}^{(N)}(t) \simeq \frac{1}{\sqrt{2\pi N p^{\uparrow\downarrow}(t)[1-p^{\uparrow\downarrow}(t)]}} \int_0^{\frac{N}{2}} dx \exp\left\{-\frac{[x-N(1-p^{\uparrow\downarrow}(t))]^2}{2Np^{\uparrow\downarrow}(t)[1-p^{\uparrow\downarrow}(t)]}\right\}. \tag{B3}$$

We can therefore write the probability $P_{\uparrow\downarrow}^{(N)}(t)$ as a difference between two error functions as

$$P_{\uparrow\downarrow}^{(N)}(t) = \frac{1}{2}\left[\mathrm{erf}\left(\frac{-\frac{N}{2}+Np^{\uparrow\downarrow}(t)}{\sqrt{2Np^{\uparrow\downarrow}(t)[1-p^{\uparrow\downarrow}(t)]}}\right) - \mathrm{erf}\left(\frac{-N+Np^{\uparrow\downarrow}(t)}{\sqrt{2Np^{\uparrow\downarrow}(t)[1-p^{\uparrow\downarrow}(t)]}}\right)\right]. \tag{B4}$$

With the explicit expression for the probabilities $P_{ij}(t)$, of which Eq. (B4) is an example, one can obtain the stationary density matrix (A1). Note that thanks to the fact that the single-spin transition probabilities satisfy $p^{\uparrow\downarrow}(t) = p^{\downarrow\uparrow}(t)$,

$$P_{\uparrow\downarrow}^{(N)}(t) = P_{\downarrow\uparrow}^{(N)}(t) \qquad \text{and} \qquad P_{\uparrow\uparrow}^{(N)}(t) = P_{\downarrow\downarrow}^{(N)}(t), \tag{B5}$$

so the symmetry in the reset-free dynamics is not restricted to the average value of the excitation density operator through $\langle n^F(t)\rangle_\uparrow = 1 - \langle n^F(t)\rangle_\downarrow$, but it is also extended to the probabilities.

In the thermodynamic limit, Eq. (B4) can be further simplified. Indeed, for $N \to \infty$, the second term tends to 1 because $p^{\uparrow\downarrow}(t) \leqslant 1$. On the other hand, the first term tends to $+1$ if $p^{\uparrow\downarrow}(t) > 1/2$ or to -1 if $p^{\uparrow\downarrow}(t) < 1/2$. Note that the number $1/2$ comes from the chosen threshold. As a consequence, the probability $P_{\uparrow\downarrow}^{(N)}(t)$ simply reduces to a Heaviside step function with a time-dependent argument,

$$P_{\uparrow\downarrow}^{(\infty)}(t) = \lim_{N\to\infty} P_{\uparrow\downarrow}^{(N)}(t) = \Theta\left[p^{\uparrow\downarrow}(t) - \frac{1}{2}\right]. \tag{B6}$$

Importantly, this result shows that $P_{\uparrow\downarrow}^{(\infty)}(t)$ can be either 1 or 0, meaning that in the thermodynamic limit, the excitation density $n = (1/N)\sum_{i=1}^N n_i$, when measured, takes deterministically a certain value, which turns out to be equal to the average value of the single-spin excitation density. This self-averaging property shows indeed that the fluctuations of n around its average value are suppressed, in accordance with the *law of large numbers*.

It is also interesting to see how the previous results change if N is assumed to be large but finite. In particular, given the large x expansion of the error function as $\mathrm{erf}x \simeq 1 - e^{-x^2}/(\sqrt{\pi}x)$, Eq. (B6) gets modified by a correction of the order of $e^{-N}/\sqrt{N}$ as

$$P_{\uparrow\downarrow}^{(N)}(t) \simeq \frac{\sqrt{2p^{\uparrow\downarrow}(t)[1-p^{\uparrow\downarrow}(t)]}}{2\sqrt{\pi N}}\left(\frac{e^{-N\frac{[\frac{1}{2}-p^{\uparrow\downarrow}(t)]^2}{2p^{\uparrow\downarrow}(t)[1-p^{\uparrow\downarrow}(t)]}}}{\frac{1}{2}-p^{\uparrow\downarrow}(t)} - \frac{e^{-N\frac{[1-p^{\uparrow\downarrow}(t)]^2}{2p^{\uparrow\downarrow}(t)[1-p^{\uparrow\downarrow}(t)]}}}{1-p^{\uparrow\downarrow}(t)}\right) \qquad \text{if } p^{\uparrow\downarrow}(t) < \frac{1}{2}, \tag{B7}$$

and

$$P_{\uparrow\downarrow}^{(N)}(t) \simeq 1 - \frac{\sqrt{2p^{\uparrow\downarrow}(t)[1-p^{\uparrow\downarrow}(t)]}}{2\sqrt{\pi N}}\left(\frac{e^{-N\frac{[\frac{1}{2}-p^{\uparrow\downarrow}(t)]^2}{2p^{\uparrow\downarrow}(t)[1-p^{\uparrow\downarrow}(t)]}}}{\frac{1}{2}-p^{\uparrow\downarrow}(t)} + \frac{e^{-N\frac{[1-p^{\uparrow\downarrow}(t)]^2}{2p^{\uparrow\downarrow}(t)[1-p^{\uparrow\downarrow}(t)]}}}{1-p^{\uparrow\downarrow}(t)}\right) \qquad \text{if } p^{\uparrow\downarrow}(t) > \frac{1}{2}. \tag{B8}$$

Note that for $N \to \infty$, one recovers the result in Eq. (B6).

Figure 3 investigates the behavior of the order parameter in Protocol II as a function of Ω/Δ for various numbers N of particles. The plotted curves are obtained with Monte Carlo simulations. In particular, we fix a large observation time T and we simulate several realizations of the reset process within this time interval by drawing the times between consecutive resets from the waiting time distribution $f(\tau)$. The average of the computed excitation density at time T over the many independent realizations of the reset process gives the numerical estimate of $\langle n\rangle_{\uparrow,\mathrm{ness}}$. This procedure is repeated for different values of Ω/Δ, leading to the result in Fig. 3. The discontinuous nonanalytic behavior of the order parameter occurring in Protocol II, and shown in Fig. 2(b) of the main text, becomes a continuous crossover when N is finite. The reason for the observed smoothening is due to the fact that for finite N, the measurement of n is no longer deterministic and does not coincide with its average value because of the statistical fluctuations encoded in Eqs. (B7) and (B8). As a consequence, even for $\Omega < \Delta$, the probability to measure $n < 1/2$ is nonzero and the system can be reset to the state $|\downarrow\rangle^N$. Because of the symmetry relation between the transition probabilities given by Eq. (B5), both coefficients $c_\uparrow$ and $c_\downarrow$ in Eq. (A1) would be equal to $1/2$, leading to a stationary value of the excitation density, computed as $\mathrm{Tr}[n\rho_{\mathrm{ness}}]$, equal to $1/2$ for any value of Ω/Δ. This is only partly captured in Fig. 3 because the exponentially small correction (B7) and (B8) to Eq. (B6) due to finite-size effects would require an

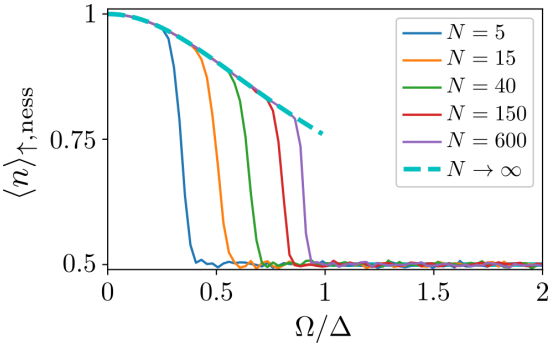

FIG. 3. Phase diagram of the (quasi)stationary excitation density in Protocol II in a finite system. The first-order phase transition that takes place in the thermodynamic limit becomes a crossover in a finite system. In this latter case, the stationary excitation density would be a constant function equal to 1/2. Due to the exponentially small finite-size corrections to Eq. (B6), only a (quasi)stationary state can be obtained numerically, which displays the expected plateau up to a certain value of Ω/Δ. The plots are obtained numerically averaging over 10 000 trajectories of the reset process. The reset rate is $\gamma = \Delta/2$ and the observation time is $T = 2000$ in units of $1/\Delta$. The dashed line, valid in the thermodynamic limit, is Eq. (3) of the main text.

exponentially long simulation to make this effect visible. In other words, obtaining numerically the stationary state for finite N becomes challenging because an exponentially large value of T is needed. Nevertheless, for small values of N, the aforementioned correction becomes larger, making the predicted plateau more visible as the crossover tends to take place at smaller values of Ω/Δ. However, since these long timescales are hardly reached in current experiments due to dissipative and incoherent effects, the curves of Fig. 3 resemble what can be realistically observed in the laboratory.

A change from the continuous nonanalytic behavior to a smooth crossover is also expected to happen in Protocol III, although the stationary excitation density would not be equal to 1/2, but would remain a decreasing function of Ω/Δ because all the possible reset states possess a positive magnetization ($n > 1/2$) and the reasoning that makes use of the symmetric relation (B5) cannot be exploited.

APPENDIX C: COMPUTATION OF THE QUANTUM DISCORD

In the main text, we compute the quantum discord of the stationary two-spin reduced density matrix, defined as

$$\rho_{jk} = \lim_{t\to\infty} \rho_{jk}(t), \tag{C1}$$

where $\rho_{jk}(t)$ is the two-spin reduced density matrix at time t. In Protocol I, it is possible to explicitly compute $\rho_{jk}(t)$ which, from Eq. (2) of the main text, is given by

$$\rho_{jk}(t) = e^{-\gamma t}\rho^F_{jk,\uparrow}(t) + \gamma \int_0^t dt' e^{-\gamma t'} \rho^F_{jk,\uparrow}(t'), \tag{C2}$$

where $\rho^F_{jk,\uparrow}(t) = \rho^F_{j,\uparrow}(t) \otimes \rho^F_{k,\uparrow}(t) = (e^{-iH_j t}\,|\uparrow\rangle_j\,\langle\uparrow|_j\,e^{iH_j t}) \otimes (e^{-iH_k t}\,|\uparrow\rangle_k\,\langle\uparrow|_k\,e^{iH_k t})$, with $H_j = \Omega\sigma^x_j + \Delta\sigma^z_j$. The stationary reduced density matrix is therefore obtained by taking the infinite time limit,

$$\rho_{jk} = \gamma \int_0^\infty dt' e^{-\gamma t'} \rho^F_{jk,\uparrow}(t'), \tag{C3}$$

which suppresses the first term of Eq. (C2). In Protocol II, instead, ρ_{jk} has two different expressions for $\Omega < \Delta$ and $\Omega > \Delta$. In particular, as also mentioned in the main text about the observable n, when $\Omega < \Delta$, its expression is the same of Eq. (C3) due to the equivalence between the two protocols. When $\Omega > \Delta$, instead, ρ_{jk} takes its most general form from Eq. (A1) and is given by two contributions, referring to the reset-free evolution from the two reset states, weighted by the coefficients $c_\uparrow$ and $c_\downarrow$ as [51]

$$\rho_{jk} = \gamma\left[c_\uparrow \int_0^\infty dt' e^{-\gamma t'} \rho^F_{jk,\uparrow}(t') + c_\downarrow \int_0^\infty dt' e^{-\gamma t'} \rho^F_{jk,\downarrow}(t')\right]. \tag{C4}$$

Because of the symmetric relation $\langle n(t)\rangle_\uparrow = 1 - \langle n(t)\rangle_\downarrow$, one has from Eq. (B5) that $c_\uparrow$ and $c_\downarrow$ in Eq. (A1) simplify as $c_\uparrow = c_\downarrow = 1/2$. This implies that the two contributions are equally weighted. This is also the reason why, for $\Omega > \Delta$, $\langle n\rangle_{\uparrow,\mathrm{ness}} = 1/2$, as explained in Appendix B.

The reduced density matrices in Eqs. (C3) and (C4) are used to compute the quantum discord for Protocol I (and Protocol II for $\Omega < \Delta$) and Protocol II (only for $\Omega > \Delta$), respectively. As mentioned in the main text, the quantum discord is quantified via the LQU, which is defined according to Ref. [69] as $l_{jk} = 1 - \lambda_{\max}\{W_{jk}\}$, where $\lambda_{\max}\{W_{jk}\}$ is the largest eigenvalue of the 3×3 matrix W_{jk} with elements $(W_{jk})_{ab} = \mathrm{Tr}[\sqrt{\rho_{jk}}(\sigma^a_j \otimes \mathbb{1})\sqrt{\rho_{jk}}(\sigma^b_j \otimes \mathbb{1})]$, with $a, b = x, y, z$.

APPENDIX D: COMPUTATION OF THE CONNECTED CORRELATION FUNCTION

In the main text, we also compute the connected correlation function between spins at sites j and k. Its stationary value is defined as

$$C^\uparrow_{jk} = \langle n_j n_k\rangle_{\uparrow,\mathrm{ness}} - \langle n_j\rangle_{\uparrow,\mathrm{ness}}\langle n_k\rangle_{\uparrow,\mathrm{ness}}\,. \tag{D1}$$

For Protocols I and II when $\Omega < \Delta$, its value is given by Eq. (4) of the main text. For Protocol II when $\Omega > \Delta$, its expression can also be exactly computed using the stationary density matrix (C4) and is given by

$$C^\uparrow_{jk} = \frac{1}{4} - 2\Omega^2 \frac{\gamma^2 - 12\Omega^2 + 16\overline{\Omega}^2}{\gamma^4 + 20\gamma^2\overline{\Omega}^2 + 64\overline{\Omega}^4}. \tag{D2}$$

This function is plotted in Fig. 2(e) of the main text.

As mentioned in Appendix A, for Protocol III, we resort to numerical Monte Carlo simulations to efficiently compute the connected correlation function and the quantum discord. We adopt the same numerical procedure described in Appendix B by simulating 80 000 independent realizations of the reset process up to the observation time $T = 30$ (in units of $1/\Delta$). The average over the reset realizations of the connected correlation function at time T is plotted, as a function of Ω/Δ, in Fig. 2(f) of the main text. Note that contrary to what has been previously observed for the estimate of $\langle n\rangle_{\uparrow,\mathrm{ness}}$, now there is no need for a very large value of T because the simulations are done in the thermodynamic limit and, therefore, one does not need a long time to reach the stationary state. What

is needed is just the dynamics of $\langle n_j^F(t) n_k^F(t)\rangle$ between two consecutive resets. In Protocol III, every state with positive magnetization ($n > 1/2$) can be considered as a reset state. Therefore, we need an expression for the reset-free dynamics of the two-point correlation function for any possible initial state with $n_0 > 1/2$. The dynamics of the order parameter is readily obtained as

$$\langle n^F(t)\rangle_{n_0} = n_0 \langle n^F(t)\rangle_{\uparrow} + (1-n_0)\langle n^F(t)\rangle_{\downarrow} \tag{D3}$$

because $N_0 = N n_0$ spins evolve starting from the $|\uparrow\rangle$ state and the remaining $N - N_0$ from the $|\downarrow\rangle$ state. For the two-point correlation function, the computation is slightly more complicated because, given an initial state with excitation density n_0, both spins at sites j and k can be initialized to $|\uparrow\rangle$ or $|\downarrow\rangle$, so four different combinations are possible. Moreover, although the probability that a *single* spin is initialized to $|\uparrow\rangle$ is exactly n_0, an analog reasoning cannot naively be applied for two spins because the event that one spin is in the excited state is clearly not independent from the state of the other spin. As a consequence, one has to follow another procedure through direct counting. In particular, since the spin pair at sites j and k can be initialized in four possible ways, given an initial state with excitation density n_0, the dynamics of the two-point correlation function until the next reset event is given by

$$\begin{aligned}\left\langle n_j^F(t) n_k^F(t)\right\rangle_{n_0} = {} & c_{\uparrow\uparrow}\langle n_j(t)^F n_k(t)^F\rangle_{\uparrow\uparrow} + c_{\uparrow\downarrow}\langle n_j(t)^F n_k(t)^F\rangle_{\uparrow\downarrow} \\ & + c_{\downarrow\uparrow}\langle n_j(t)^F n_k(t)^F\rangle_{\downarrow\uparrow} \\ & + c_{\downarrow\downarrow}\langle n_j(t)^F n_k(t)^F\rangle_{\downarrow\downarrow},\end{aligned} \tag{D4}$$

where the coefficients c_{ab} are the probabilities to find the spin at site j initialized in the state $|a\rangle$ and the spin at site k initialized in the state $|b\rangle$, given that the system has excitation density n_0. In order to compute these probabilities, let us first count the number of possible spin configurations which give a total excitation density equal to $n_0 = N_0/N$. This is given by $\binom{N}{N_0}$. The number of configurations in which both spins at sites j and k are in the excited state is obtained by counting the possible ways to arrange the remaining $N_0 - 2$ up spins among the remaining $N - 2$ sites. Since this number is simply given by $\binom{N-2}{N_0-2}$, the first coefficient entering Eq. (D4) reads

$$c_{\uparrow\uparrow} = \binom{N-2}{N_0-2}\Big/\binom{N}{N_0} = \frac{N_0(N_0-1)}{N(N-1)}. \tag{D5}$$

Analogously, the other coefficients are given by

$$\begin{aligned} c_{\uparrow\downarrow} &= \binom{N-2}{N_0-1}\Big/\binom{N}{N_0} = \frac{N_0(N-N_0)}{N(N-1)}, \\ c_{\downarrow\uparrow} &= c_{\uparrow\downarrow}, \\ c_{\downarrow\downarrow} &= \binom{N-2}{N_0}\Big/\binom{N}{N_0} = \frac{(N-N_0)(N-N_0-1)}{N(N-1)}. \end{aligned} \tag{D6}$$

One can check that the coefficients normalize to 1, i.e., $c_{\uparrow\uparrow} + c_{\uparrow\downarrow} + c_{\downarrow\uparrow} + c_{\downarrow\downarrow} = 1$. By taking the thermodynamic limit $N \to \infty$, their dependence on N disappears and they reduce to

$$\begin{aligned} c_{\uparrow\uparrow} &= n_0^2, \\ c_{\uparrow\downarrow} &= c_{\downarrow\uparrow} = n_0(1-n_0), \\ c_{\downarrow\downarrow} &= (1-n_0)^2, \end{aligned} \tag{D7}$$

showing that the thermodynamic limit eliminates the statistical dependence between the state of the spin at site j and the one of the spin at site k. One can then easily obtain the dynamics of the correlation function by inserting these coefficients in Eq. (D4) and exploiting the factorization $\langle n_j^F(t) n_k^F(t)\rangle = \langle n_j^F(t)\rangle\langle n_k^F(t)\rangle$ as a result of the fact that the spins do not interact. The quantum discord, plotted in Fig. 2(f) of the main text as a function of Ω/Δ, is obtained numerically in an analogous way by simulating 20 000 independent realizations of the reset process up to the observation time $T = 30$ (in units of $1/\Delta$). Specifically, one needs the dynamics $\rho_{jk}^F(t)_{n_0}$ of the two-spin reduced density matrix between two consecutive resets. The dynamics $\rho_{jk}^F(t)_{n_0}$ is then written analogously as in Eq. (D4) in terms of the reset-free dynamics $\rho_{jk}^F(t)_{ab}$, where the spins j and k are initialized in the state $|a\rangle$ and $|b\rangle$, respectively. The coefficients c_{ab} of the four terms in the sum are again given in Eq. (D7).

APPENDIX E: NON-POISSONIAN RESETTING

In the main text and in the previous sections, we focus on the Poissonian resetting, where the waiting time distribution is an exponential function. To account for the finite coherence time attained in cold-atom systems, a more suitable waiting time distribution would, however, be of the form of a "chopped exponential" [51],

$$f(t) = \frac{\gamma}{1-e^{-\gamma t_{\max}}} e^{-\gamma t}\,\Theta(t_{\max}-t), \tag{E1}$$

where $t_{\max}$ is the maximum reset time. The survival probability then reads

$$q(t) = \frac{e^{-\gamma t} - e^{-\gamma t_{\max}}}{1-e^{-\gamma t_{\max}}}\,\Theta(t_{\max}-t). \tag{E2}$$

The non-Poissonian case of Eqs. (E1) and (E2) does not bear any additional conceptual difficulty with respect to the Poissonian one and it can be analyzed along the same lines using Eq. (A1) [which is indeed valid for an arbitrary waiting time distribution $f(t)$ and survival probability $q(t)$]. For Protocol I, the stationary density matrix ρ_{ness} is obtained from the limiting form of Eq. (A1) with $c_\uparrow = 1$ and $c_\downarrow = 0$, as explained in Appendix A.

The results remain qualitatively the same as in the Poissonian case, with the appearance of a discontinuous and a continuous nonanalytic behavior of the order parameter at the same critical point $\Omega_c = \Delta$ in Protocols II and III, respectively. This is, in particular, true as long as $t_{\max}$ is large enough compared to Ω^{-1} to allow for the magnetization to change sign in the regime $\Omega > \Delta$. If this is not the case, then all the protocols reduce to Protocol I. The properties of the correlation function and the quantum discord also remain unchanged. As an example, here we report the expression of

the stationary excitation density $\langle n\rangle_{\uparrow,\mathrm{ness}}$ for $\Omega < \Delta$ as

$$\langle n\rangle_{\uparrow,\mathrm{ness}} = 1 - \frac{\Omega^2}{2\overline{\Omega}^2(\gamma^2+4\overline{\Omega}^2)}\left\{4\overline{\Omega}^2 - \frac{\gamma^2}{e^{\gamma t_{\max}}-1-\gamma t_{\max}}\left[2\sin^2(\overline{\Omega}t_{\max}) - \frac{\gamma}{\overline{\Omega}}\sin(\overline{\Omega}t_{\max})\cos(\overline{\Omega}t_{\max}) + \gamma t_{\max}\right]\right\}, \quad \text{(E3)}$$

which reduces to Eq. (3) of the main text for $t_{\max} \to \infty$.

[1] M. Born, Quantenmechanik der Stoßvorgänge, Z. Phys. **38**, 803 (1926).

[2] N. Bohr, The quantum postulate and the recent development of atomic theory, Nature (London) **121**, 580 (1928).

[3] G. Lindblad, On the generators of quantum dynamical semigroups, Commun. Math. Phys. **48**, 119 (1976).

[4] V. Gorini, A. Kossakowski, and E. C. G. Sudarshan, Completely positive dynamical semigroups of *N*-level systems, J. Math. Phys. **17**, 821 (1976).

[5] C. Gardiner and P. Zoller, *Quantum Noise: A Handbook of Markovian and non-Markovian Quantum Stochastic Methods with Applications to Quantum Optics*, Springer Series in Synergetics (Springer, New York, 2004).

[6] H.-P. Breuer and F. Petruccione, *The Theory of Open Quantum Systems* (Oxford University Press, Oxford, 2007).

[7] H. M. Wiseman, Quantum theory of continuous feedback, Phys. Rev. A **49**, 2133 (1994).

[8] H. M. Wiseman and G. J. Milburn, *Quantum Measurement and Control* (Cambridge University Press, Cambridge, 2009).

[9] K. Jacobs, *Quantum Measurement Theory and its Applications* (Cambridge University Press, Cambridge, 2014).

[10] J. Lammers, H. Weimer, and K. Hammerer, Open-system many-body dynamics through interferometric measurements and feedback, Phys. Rev. A **94**, 052120 (2016).

[11] H. Nurdin and N. Yamamoto, *Linear Dynamical Quantum Systems: Analysis, Synthesis, and Control* (Springer International, New York, 2017).

[12] K. Kroeger, N. Dogra, R. Rosa-Medina, M. Paluch, F. Ferri, T. Donner, and T. Esslinger, Continuous feedback on a quantum gas coupled to an optical cavity, New J. Phys. **22**, 033020 (2020).

[13] D. A. Ivanov, T. Y. Ivanova, S. F. Caballero-Benitez, and I. B. Mekhov, Feedback-Induced Quantum Phase Transitions Using Weak Measurements, Phys. Rev. Lett. **124**, 010603 (2020).

[14] G. Buonaiuto, F. Carollo, B. Olmos, and I. Lesanovsky, Dynamical Phases and Quantum Correlations in an Emitter-Waveguide System with Feedback, Phys. Rev. Lett. **127**, 133601 (2021).

[15] D. A. Ivanov, T. Y. Ivanova, S. F. Caballero-Benitez, and I. B. Mekhov, Tuning the universality class of phase transitions by feedback: Open quantum systems beyond dissipation, Phys. Rev. A **104**, 033719 (2021).

[16] J. T. Young, A. V. Gorshkov, and I. B. Spielman, Feedback-stabilized dynamical steady states in the Bose-Hubbard model, Phys. Rev. Res. **3**, 043075 (2021).

[17] M. R. Evans, S. N. Majumdar, and G. Schehr, Stochastic resetting and applications, J. Phys. A: Math. Theor. **53**, 193001 (2020).

[18] M. R. Evans and S. N. Majumdar, Diffusion with Stochastic Resetting, Phys. Rev. Lett. **106**, 160601 (2011).

[19] M. R. Evans and S. N. Majumdar, Diffusion with optimal resetting, J. Phys. A: Math. Theor. **44**, 435001 (2011).

[20] M. R. Evans and S. N. Majumdar, Diffusion with resetting in arbitrary spatial dimension, J. Phys. A: Math. Theor. **47**, 285001 (2014).

[21] S. N. Majumdar, S. Sabhapandit, and G. Schehr, Dynamical transition in the temporal relaxation of stochastic processes under resetting, Phys. Rev. E **91**, 052131 (2015).

[22] L. Kusmierz, S. N. Majumdar, S. Sabhapandit, and G. Schehr, First Order Transition for the Optimal Search Time of Lévy Flights with Resetting, Phys. Rev. Lett. **113**, 220602 (2014).

[23] A. Pal and S. Reuveni, First Passage under Restart, Phys. Rev. Lett. **118**, 030603 (2017).

[24] A. Chechkin and I. M. Sokolov, Random Search with Resetting: A Unified Renewal Approach, Phys. Rev. Lett. **121**, 050601 (2018).

[25] M. Radice, Diffusion processes with Gamma-distributed resetting and non-instantaneous returns, J. Phys. A: Math. Theor. **55**, 224002 (2022).

[26] M. R. Evans, S. N. Majumdar, and K. Mallick, Optimal diffusive search: Nonequilibrium resetting versus equilibrium dynamics, J. Phys. A: Math. Theor. **46**, 185001 (2013).

[27] C. Christou and A. Schadschneider, Diffusion with resetting in bounded domains, J. Phys. A: Math. Theor. **48**, 285003 (2015).

[28] A. B. Slowman, M. R. Evans, and R. A. Blythe, Jamming and Attraction of Interacting Run-and-Tumble Random Walkers, Phys. Rev. Lett. **116**, 218101 (2016).

[29] M. R. Evans and S. N. Majumdar, Run and tumble particle under resetting: A renewal approach, J. Phys. A: Math. Theor. **51**, 475003 (2018).

[30] V. Kumar, O. Sadekar, and U. Basu, Active Brownian motion in two dimensions under stochastic resetting, Phys. Rev. E **102**, 052129 (2020).

[31] I. Santra, U. Basu, and S. Sabhapandit, Run-and-tumble particles in two dimensions under stochastic resetting conditions, J. Stat. Mech. (2020) 113206.

[32] P. C. Bressloff, Modeling active cellular transport as a directed search process with stochastic resetting and delays, J. Phys. A: Math. Theor. **53**, 355001 (2020).

[33] S. Gupta, S. N. Majumdar, and G. Schehr, Fluctuating Interfaces Subject to Stochastic Resetting, Phys. Rev. Lett. **112**, 220601 (2014).

[34] S. Eule and J. J. Metzger, Non-equilibrium steady states of stochastic processes with intermittent resetting, New J. Phys. **18**, 033006 (2016).

[35] V. Méndez and D. Campos, Characterization of stationary states in random walks with stochastic resetting, Phys. Rev. E **93**, 022106 (2016).

[36] P. Grange, Non-conserving zero-range processes with extensive rates under resetting, J. Phys. Commun. **4**, 045006 (2020).

[37] M. Magoni, S. N. Majumdar, and G. Schehr, Ising model with stochastic resetting, Phys. Rev. Res. **2**, 033182 (2020).
[38] C. Aron and M. Kulkarni, Nonanalytic nonequilibrium field theory: Stochastic reheating of the Ising model, Phys. Rev. Res. **2**, 043390 (2020).
[39] W. Wang, A. G. Cherstvy, H. Kantz, R. Metzler, and I. M. Sokolov, Time averaging and emerging nonergodicity upon resetting of fractional Brownian motion and heterogeneous diffusion processes, Phys. Rev. E **104**, 024105 (2021).
[40] V. Stojkoski, T. Sandev, L. Kocarev, and A. Pal, Geometric Brownian motion under stochastic resetting: A stationary yet nonergodic process, Phys. Rev. E **104**, 014121 (2021).
[41] I. Santra, S. Das, and S. K. Nath, Brownian motion under intermittent harmonic potentials, J. Phys. A: Math. Theor. **54**, 334001 (2021).
[42] F. Huang and H. Chen, Random walks on complex networks with first-passage resetting, Phys. Rev. E **103**, 062132 (2021).
[43] K. Goswami and R. Chakrabarti, Stochastic resetting and first arrival subjected to Gaussian noise and Poisson white noise, Phys. Rev. E **104**, 034113 (2021).
[44] P. Chełminiak, Non-linear diffusion with stochastic resetting, J. Phys. A: Math. Theor. **55**, 384004 (2022).
[45] L. Hartmann, W. Dür, and H.-J. Briegel, Steady-state entanglement in open and noisy quantum systems, Phys. Rev. A **74**, 052304 (2006).
[46] N. Linden, S. Popescu, and P. Skrzypczyk, How Small Can Thermal Machines Be? The Smallest Possible Refrigerator, Phys. Rev. Lett. **105**, 130401 (2010).
[47] A. Tavakoli, G. Haack, N. Brunner, and J. B. Brask, Autonomous multipartite entanglement engines, Phys. Rev. A **101**, 012315 (2020).
[48] B. Mukherjee, K. Sengupta, and S. N. Majumdar, Quantum dynamics with stochastic reset, Phys. Rev. B **98**, 104309 (2018).
[49] D. C. Rose, H. Touchette, I. Lesanovsky, and J. P. Garrahan, Spectral properties of simple classical and quantum reset processes, Phys. Rev. E **98**, 022129 (2018).
[50] F. Carollo, R. L. Jack, and J. P. Garrahan, Unraveling the Large Deviation Statistics of Markovian Open Quantum Systems, Phys. Rev. Lett. **122**, 130605 (2019).
[51] G. Perfetto, F. Carollo, M. Magoni, and I. Lesanovsky, Designing nonequilibrium states of quantum matter through stochastic resetting, Phys. Rev. B **104**, L180302 (2021).
[52] A. Riera-Campeny, J. Ollé, and A. Masó-Puigdellosas, Measurement-induced resetting in open quantum systems, arXiv:2011.04403.
[53] X. Turkeshi, M. Dalmonte, R. Fazio, and M. Schirò, Entanglement transitions from stochastic resetting of non-Hermitian quasiparticles, Phys. Rev. B **105**, L241114 (2022).
[54] D. Das, S. Dattagupta, and S. Gupta, Quantum unitary evolution interspersed with repeated non-unitary interactions at random times: The method of stochastic Liouville equation, and two examples of interactions in the context of a tight-binding chain, J. Stat. Mech. (2022) 053101.
[55] G. Perfetto, F. Carollo, and I. Lesanovsky, Thermodynamics of quantum-jump trajectories of open quantum systems subject to stochastic resetting, SciPost Phys. **13**, 079 (2022).
[56] M. Raghunandan, J. Wrachtrup, and H. Weimer, High-Density Quantum Sensing with Dissipative First Order Transitions, Phys. Rev. Lett. **120**, 150501 (2018).
[57] L.-P. Yang and Z. Jacob, Quantum critical detector: Amplifying weak signals using discontinuous quantum phase transitions, Opt. Express **27**, 10482 (2019).
[58] Y. Chu, S. Zhang, B. Yu, and J. Cai, Dynamic Framework for Criticality-Enhanced Quantum Sensing, Phys. Rev. Lett. **126**, 010502 (2021).
[59] I. M. Georgescu, S. Ashhab, and F. Nori, Quantum simulation, Rev. Mod. Phys. **86**, 153 (2014).
[60] M. Endres, H. Bernien, A. Keesling, H. Levine, E. Anschuetz, A. Krajenbrink, C. Senko, V. Vuletic, M. Greiner, and M. Lukin, Atom-by-atom assembly of defect-free one-dimensional cold atom arrays, Science **354**, 1024 (2016).
[61] D. Barredo, S. Léséleuc, V. Lienhard, T. Lahaye, and A. Browaeys, An atom-by-atom assembler of defect-free arbitrary 2D atomic arrays, Science **354**, 1021 (2016).
[62] C. Robens, J. Zopes, W. Alt, S. Brakhane, D. Meschede, and A. Alberti, Low-Entropy States of Neutral Atoms in Polarization-Synthesized Optical Lattices, Phys. Rev. Lett. **118**, 065302 (2017).
[63] L. Henriet, L. Beguin, A. Signoles, T. Lahaye, A. Browaeys, G.-O. Reymond, and C. Jurczak, Quantum computing with neutral atoms, Quantum **4**, 327 (2020).
[64] B. Misra and E. C. G. Sudarshan, The Zeno's paradox in quantum theory, J. Math. Phys. **18**, 756 (1977).
[65] C. B. Chiu, E. C. G. Sudarshan, and B. Misra, Time evolution of unstable quantum states and a resolution of Zeno's paradox, Phys. Rev. D **16**, 520 (1977).
[66] F. Benatti, F. Carollo, R. Floreanini, and H. Narnhofer, Quantum spin chain dissipative mean-field dynamics, J. Phys. A: Math. Theor. **51**, 325001 (2018).
[67] F. Benatti, F. Carollo, R. Floreanini, and H. Narnhofer, Non-Markovian mesoscopic dissipative dynamics of open quantum spin chains, Phys. Lett. A **380**, 381 (2016).
[68] M. Buchhold, Y. Minoguchi, A. Altland, and S. Diehl, Effective Theory for the Measurement-Induced Phase Transition of Dirac Fermions, Phys. Rev. X **11**, 041004 (2021).
[69] D. Girolami, T. Tufarelli, and G. Adesso, Characterizing Nonclassical Correlations via Local Quantum Uncertainty, Phys. Rev. Lett. **110**, 240402 (2013).
[70] H. Ollivier and W. H. Zurek, Quantum Discord: A Measure of the Quantumness of Correlations, Phys. Rev. Lett. **88**, 017901 (2001).
[71] L. Henderson and V. Vedral, Classical, quantum and total correlations, J. Phys. A: Math. Gen. **34**, 6899 (2001).
[72] A. Ferraro, L. Aolita, D. Cavalcanti, F. M. Cucchietti, and A. Acín, Almost all quantum states have nonclassical correlations, Phys. Rev. A **81**, 052318 (2010).
[73] K. Modi, H. Cable, M. Williamson, and V. Vedral, Quantum Correlations in Mixed-State Metrology, Phys. Rev. X **1**, 021022 (2011).
[74] D. Girolami, A. M. Souza, V. Giovannetti, T. Tufarelli, J. G. Filgueiras, R. S. Sarthour, D. O. Soares-Pinto, I. S. Oliveira, and G. Adesso, Quantum Discord Determines the Interferometric Power of Quantum States, Phys. Rev. Lett. **112**, 210401 (2014).
[75] A. Sone, Q. Zhuang, and P. Cappellaro, Quantifying precision loss in local quantum thermometry via diagonal discord, Phys. Rev. A **98**, 012115 (2018).
[76] C. G. Wade, M. Marcuzzi, E. Levi, J. M. Kondo, I. Lesanovsky, C. S. Adams, and K. J. Weatherill, A terahertz-driven nonequi-

librium phase transition in a room temperature atomic vapour, Nat. Commun. **9**, 3567 (2018).

[77] Y.-Y. Jau and T. Carter, Vapor-Cell-Based Atomic Electrometry for Detection Frequencies below 1 kHz, Phys. Rev. Appl. **13**, 054034 (2020).

[78] L. A. Downes, A. R. MacKellar, D. J. Whiting, C. Bourgenot, C. S. Adams, and K. J. Weatherill, Full-Field Terahertz Imaging at Kilohertz Frame Rates Using Atomic Vapor, Phys. Rev. X **10**, 011027 (2020).

[79] S. Hollerith, J. Zeiher, J. Rui, A. Rubio-Abadal, V. Walther, T. Pohl, D. M. Stamper-Kurn, I. Bloch, and C. Gross, Quantum gas microscopy of Rydberg macrodimers, Science **364**, 664 (2019).

[80] W. Feller, *An Introduction to Probability Theory and its Applications* (Wiley, New York, 1968).